

Critical scaling and type-III intermittent chaos in isolated rabbit resistance arteries

T. M. Griffith,* D. Parthimos, J. Crombie, and D. H. Edwards

Cardiovascular Sciences Research Group, Department of Diagnostic Radiology, University of Wales College of Medicine, Heath Park, Cardiff CF4 4XN, United Kingdom

(Received 19 May 1997; revised manuscript received 13 August 1997)

We have shown that spontaneous oscillations in flow in rabbit ear resistance arteries may sometimes exhibit behavior typical of type-III Pomeau-Manneville intermittency. The average number of oscillations per laminar length $\langle n \rangle$ was related to a bifurcation parameter ε according to power-law scaling of the form $\langle n \rangle \sim \varepsilon^{-\beta}$. The critical exponent β was estimated as ~ 0.80 , which is within the range reported for type-III intermittent chaos in nonbiological systems. [S1063-651X(97)50412-0]

PACS number(s): 87.10.+e

Spontaneous fluctuations in vascular tone (vasomotion) are ubiquitous in the microcirculation and are thought to confer physiological benefit by enhancing mass transport processes, promoting lymphatic drainage, and helping to sustain distal tissue perfusion when supply pressure is low (e.g., during haemorrhagic shock) [1–3]. Previous studies from this laboratory have shown that the mechanisms underlying vasomotion in rabbit ear arteries perfused with histamine can be classified as chaotic [4–6]. We now provide evidence that this intrinsic nonlinearity may generate patterns of intermittent chaos in which irregular bursts interrupt an otherwise periodic signal (Fig. 1). Experiments were performed on isolated first generation ear arteries, ~ 1 cm in length and $\sim 150 \mu\text{m}$ in diameter, from male New Zealand White rabbits sacrificed by intravenous injection of sodium pentobarbitone (120 mg kg^{-1}), as previously described [4–6].

Pomeau and Manneville have described three “universal” intermittency classes in which the essential features of intermittent chaos are captured by discrete one-dimensional iterative maps [7–9]. Each of these classes corresponds uniquely to the manner in which the eigenvalues of a fixed point pass through the unit circle at a local bifurcation, and each exhibits different scaling characteristics in terms of the theoretical relationship between the average number of oscillations per laminar segment and a bifurcation parameter. In the type-III scenario, intermittent laminar dynamics arises through the destabilization of a limit cycle via a subcritical period-doubling bifurcation that leads to an expansion in the amplitude of one subharmonic mode and a simultaneous contraction in another. Ultimately the dynamics loses regularity and a chaotic burst appears, following which there is a return to the preceding periodic behavior. This highly specific antithetic divergence of modes has previously been observed in semiconductors [10,11], lasers [12], and electrical circuits [13], and at the onset of fluid turbulence [14], but not to our knowledge in biological systems. Following Pomeau and Manneville we have constructed the second return map describing successive maxima x_n in the fluctuations in flow observed in rabbit ear arteries according to

$$x_{n+2} = (1 + 2\varepsilon)x_n + bx_n^3, \quad (1)$$

where ε is a small bifurcation parameter and b is a constant such that the monophasic regime is represented by a repelling unstable fixed point. Two examples of return maps derived from such experimental signals are illustrated in Fig. 2, for which least-squares fits yielded $\varepsilon \sim 0.12$ and ~ 0.15 , respectively.

In type-III intermittency, the number of iterations n undertaken by a representative trajectory before it exits from the laminar channel of the cubic map at $x_n = c$ depends on the distance from the unstable monophasic point x_0 at which reinjection occurs after the previous chaotic burst, and can be calculated by approximating Eq. (1) in the continuous form [9,14]

$$\frac{dx}{dn} = 2\varepsilon x + bx^3. \quad (2)$$

If $\varepsilon \sim 0$ and c is large, integration leads to

$$n(\varepsilon, x_0) \sim \frac{1}{\varepsilon} \ln \left(\frac{2\varepsilon + bx_0^2}{x_0^2} \right). \quad (3)$$

If it is assumed that reinjection occurs uniformly over the interval $[0, c]$, the cumulative probability distribution for the number of laminar segments with more than n_0 oscillations is given by [9,10,12]

$$N(n_0) = \int_{n_0}^{\infty} P(n) dn = \int_0^c P(x_0) \frac{dx_0}{dn} dn \\ \sim \varepsilon^{3/2} \frac{\exp(-2\varepsilon n_0)}{[1 - \exp(-4\varepsilon n_0)]^{1/2}}. \quad (4)$$

This probability distribution can be used to distinguish between the different Pomeau-Manneville intermittency classes [10,12], and in the present study confirms that the observed distributions of $N(n_0)$ for arteries exhibiting intermittency over periods ~ 90 minutes or longer are consistent with classification as type-III (Fig. 3). Equation (4) thus permits the calculation of an average value of ε over a complete experiment from the distribution of the lengths of each of the laminar phases of the dynamics. Since reinjection occurs at a

*Author to whom correspondence should be addressed. FAX: 01222-74426. Electronic address: Griffith@Cardiff.AC.UK

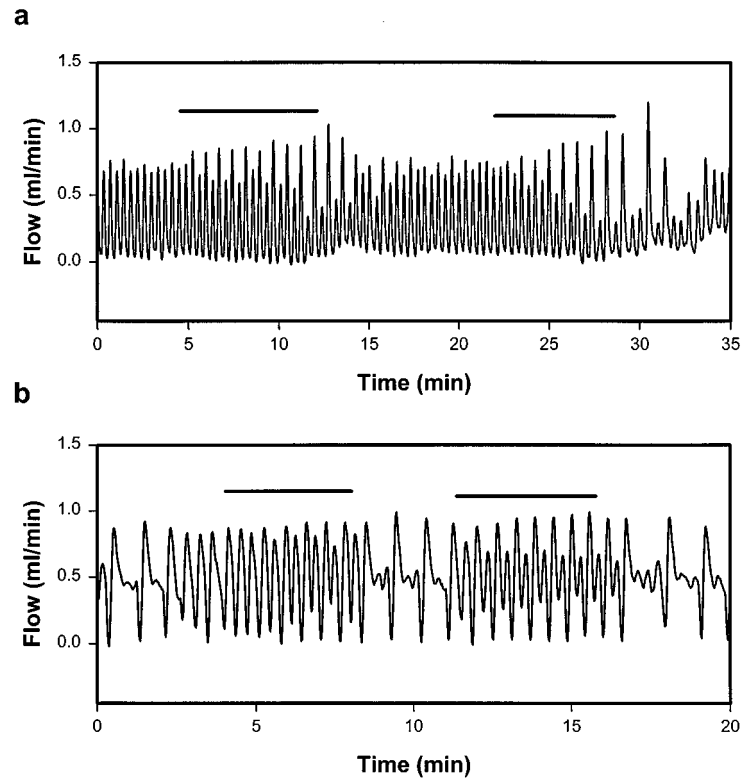


FIG. 1. Flow oscillations observed in two isolated rabbit arteries following administration of $2.5 \mu\text{M}$ histamine. Mean flow was maintained at 0.5 ml/min by setting the speed of the pump that controlled perfusion, and fluctuations in flow monitored continuously by a transonic flow probe (Transonic Systems, type 2N). Both examples illustrate features typical of the subharmonic bifurcation that characterizes type-III Pomeau-Manneville intermittency. (a) Trace obtained in the presence of $50 \mu\text{M}$ N^G -nitro- L -arginine methyl ester to inhibit nitric oxide synthesis by the vascular endothelium. The flow maxima show divergence with baseline flow remaining almost constant. (b) Trace obtained in the presence of histamine alone, in which diverging modes can be identified in the net amplitude of the flow excursion. Segments identified by horizontal bars conform to the criteria used to define the laminar phases of the dynamics (see text).

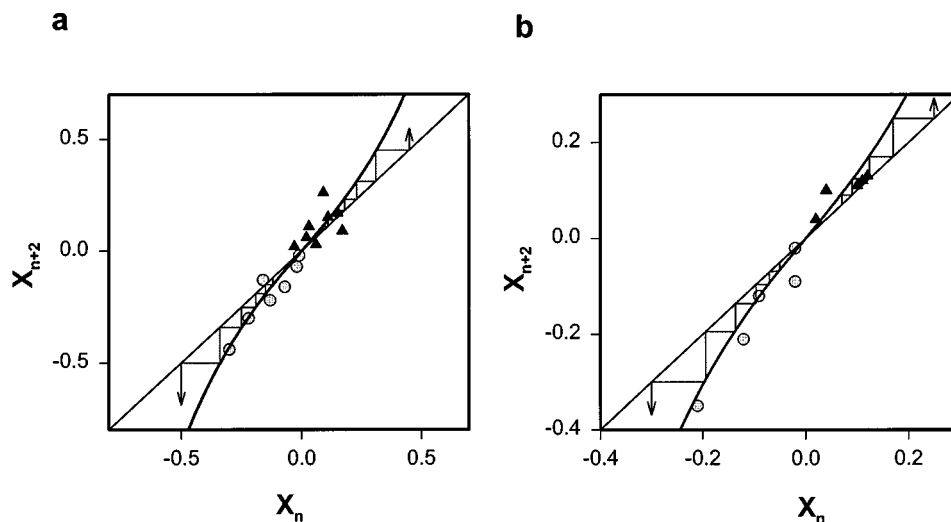


FIG. 2. Second return maps constructed from experimental signals. (a) Plots of successive maxima in the fluctuations in flow for the second segment identified by a horizontal bar in Fig. 1(a). Circles represent the contracting mode and triangles the expanding mode as the dynamics evolves over time away from the “ghost” of the monopercodic regime, i.e., the fixed point $x_{n+2} = x_n$. (b) Plots of successive flow excursions (i.e., maxima-minima) for the first segment identified by a horizontal bar in Fig. 1(b). Both maps were fitted by an expression of the form $x_{n+2} = (1 + 2\varepsilon)x_n + bx_n^3$, with (a) $\varepsilon = 0.12$, $b = 2.07$ and (b) $\varepsilon = 0.15$, $b = 5.62$. x_n denotes deviation from the fixed point, which corresponded experimentally to flows of ~ 0.70 and $\sim 0.78 \text{ ml min}^{-1}$, respectively. As illustrated schematically, the laminar phase of type-III intermittency ends when the dynamics is ejected from the map. Standard theory assumes that reinjection takes place in the vicinity of the fixed point with a uniform random probability distribution, allowing the process to repeat.

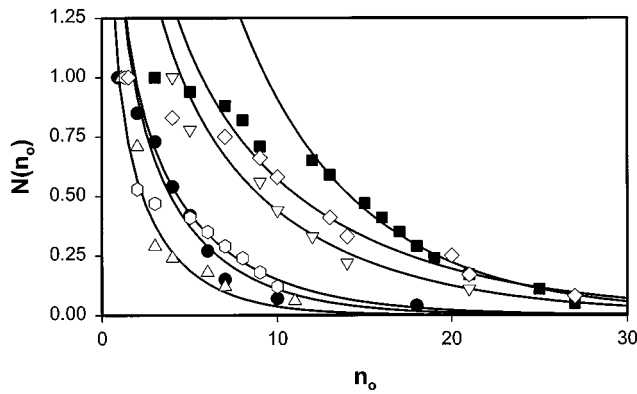


FIG. 3. Cumulative probability distributions representing the normalized fraction of intermittent laminar segments longer than n_0 oscillatory excursions for six arteries exhibiting type-III intermittency whose behavior appeared stable for periods of at least 90 min. Individual symbols denote experimental data and continuous lines the best fit to the theoretical expression that characterizes this intermittency class, i.e., $N(n_0) \sim \exp(-2\epsilon n_0)[1 - \exp(-4\epsilon n_0)]^{1/2}$ (see text). Open symbols denote arteries perfused with histamine alone; closed symbols denote the additional presence of N^G -nitro-*L*-arginine methyl ester to inhibit endothelial nitric oxide (NO) synthesis. Long laminar lengths reflect the local structure of the cubic map near the unstable fixed point, whereas short laminar lengths correspond to reinjections far away from this point and principally reflect the dynamics of reinjection, which standard theory does not take into account. To ensure evaluation of the ‘‘optimal’’ decay region of Eq. (4), therefore, short laminar lengths were in some cases excluded from the curve fitting procedure, as discussed in Ref. [10].

finite distance from the unstable fixed point, the two subharmonic modes always diverge with unequal starting amplitudes (e.g., Fig. 1(b), see also Refs. [13, 14]). Therefore, in order to identify the reinjection point for a given orbit, and thus define the onset of the laminar phase, the two subharmonic modes were tracked backwards in time from the end of the laminar phase to the point at which their amplitudes showed closest convergence. Termination of the laminar phase was defined as loss of the characteristic antithetic divergence of the modes for more than two cycles, followed by irregular behavior. In order to evaluate the possible consequences of systematic errors introduced by the adoption of these criteria, we varied the estimated laminar lengths either by deletion or addition of up to four cycles. This did not alter values of ϵ calculated using Eq. (4) by more than 10%.

The duration of the laminar phase in type-III intermittency increases as the bifurcation parameter $\epsilon \rightarrow 0$, so that the inverse average laminar length $\langle n \rangle^{-1}$ plays the role of an order parameter characterizing a critical phenomenon. ϵ may thus be considered as a displacement from a critical point according to

$$\epsilon = \frac{\mu - \mu_c}{\mu_c}, \quad (5)$$

where μ is a fundamental control parameter and μ_c its value at the critical point marking the onset of intermittency. In physical systems exhibiting type-III intermittency μ has been

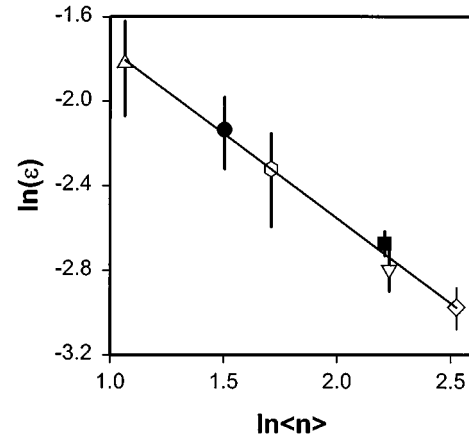


FIG. 4. Relationship between the average number of oscillations per laminar segment and the bifurcation parameter ϵ . Error bars were derived from the fitted curves of Fig. 3 (with the symbols corresponding). The linearity of this plot is consistent with scaling according to $\langle n \rangle \sim \epsilon^{-\beta}$ where β is a critical exponent. Regression analysis gave the value $\beta = 0.80 \pm 0.04$ ($r = 0.99$).

directly related to a variable such as magnetic-field strength or resistance that can be altered experimentally in a graded fashion to demonstrate critical scaling, with ϵ derived either from a second return map or a cumulative probability distribution [10,12,13]. Although the nature of the putative control parameter μ in the present physiological experiments is unknown, and cannot, therefore, be manipulated in a controlled fashion, it has still been possible to demonstrate scaling by analyzing the intermittent behavior of a series of individual arteries. Logarithmic plots of mean laminar length $\langle n \rangle$ as a function of the derived bifurcation parameter ϵ thus revealed a power-law relationship of the form $\langle n \rangle \sim \epsilon^{-\beta}$ with an estimated value of $\beta \sim 0.80$ (Fig. 4).

It is widely recognized that the vascular endothelium contributes to the regulation of arterial resistance by releasing the potent endogenous vasodilator nitric oxide NO in response to changes in flow and circulating hormones. In the present experiments we observed type-III intermittency in a total of 19 different arteries but its existence did not correlate with the presence or absence of 50 μM N^G -nitro-*L*-arginine methyl ester, a compound that blocks NO synthesis. Furthermore, in those preparations that exhibited intermittent behavior for periods of time sufficiently long to permit derivation of ϵ from a cumulative probability distribution, critical scaling did not appear to be influenced by this inhibitor (Fig. 4). The role of NO may consequently be regarded as modulatory rather than essential, a view supported by correlation dimension analysis, which has shown that NO does not influence the intrinsic complexity of rabbit artery vasomotion [4].

The value of β estimated for rabbit ear artery vasomotion is close to that reported for current fluctuations in liquid-He-cooled ultrapure crystals of germanium near the threshold for spontaneous instability (0.85) [11]. Others, however, have obtained $\beta \sim 1.2$ for electrical oscillations associated with the low-temperature avalanche breakdown of *p*-type germanium subjected to a variable magnetic field [10], and $\beta \sim 0.55$ in a negative resistance electronic circuit [13]. It is readily seen from Eq. (3) that $n(\epsilon) \sim 1/\epsilon$ when $x_0^2 \gg \epsilon$, which suggests $\beta = 1$ as discussed in Refs. [9] and [15]. Kodama, Sato, and

Honda [16], however, used a renormalization group approach to obtain $\beta=0.5$ for the expected average laminar length. This varies as

$$\langle n \rangle = \int_1^\infty nP(n)dn \sim \varepsilon^{-1/2} \int_\varepsilon^\infty \frac{x \exp(-2x)}{[1 - \exp(-4x)]^{3/2}} dx, \quad (6)$$

with the substitution $x = \varepsilon n$. Convergence of this integral is assured numerically in the limit $\varepsilon \rightarrow 0$ consistent with $\beta=0.5$ [16]. The theoretical value of the scaling exponent for type-III intermittency has thus itself become the subject of controversy.

Major temporal fluctuations in regional perfusion within the ear microcirculation of conscious rabbits were first described in detail by Clark and Clark in 1932, and shown to result from the asynchronous opening and closing of arteries in different parts of the vascular network on time scales similar to those observed in the present study [17]. This phenomenon has been noted in many other vascular beds and may serve to ensure that all microregions ultimately receive perfusion by temporarily impeding local flow and causing blood to be conducted to alternative tissue elements. The arteries

employed in the present study may be considered as a spatially extended system consisting of a large number of coupled cells [18], and Kahn, Mar, and Westervelt [11] have also identified type-III intermittency in the spatiotemporal dynamics of a physical system possessing many degrees of freedom. Correlation dimension analysis has also shown that the dynamics of rabbit ear artery vasomotion is at least four dimensional [4–6]. It is thus apparent that the “macroscopic” behavior of complex systems can collapse to relatively simple patterns that exhibit critical behavior. In the context of vasomotion this could confer flexibility by allowing the “intermittent” redistribution of flow observed *in vivo* to remain at the “edge of chaos” under the control of a single parameter that effectively generates a switching mechanism. Chaotic regulation may optimize microcirculatory function relative to simple oscillatory control by accelerating diffusion-limited mass transport processes, rapidly dissipating transients, and may allow large changes in state to occur with minimal energy expenditure [6,19,20].

The work was supported by the Medical Research Council.

-
- [1] J. A. Schmidt, M. Intaglietta, and P. J. Borgström, *J. Appl. Physiol.* **73**, 1077 (1992).
- [2] T. W. Secomb, M. Intaglietta, and J. F. Gross, *Prog. Appl. Microcirc.* **15**, 49 (1989).
- [3] T. C. Skalak, G. W. Schmid-Schönbein, and B. W. Zweifach, *Microvasc. Res.* **28**, 95 (1984).
- [4] T. M. Griffith and D. H. Edwards, *Am. J. Physiol.* **266**, H1786 (1994).
- [5] T. M. Griffith and D. H. Edwards, *Am. J. Physiol.* **266**, H1801 (1994).
- [6] T. M. Griffith and D. H. Edwards, *Am. J. Physiol.* **269**, H656 (1995).
- [7] P. Manneville and Y. Pomeau, *Physica D* **1**, 219 (1980).
- [8] Y. Pomeau and P. Manneville, *Commun. Math. Phys.* **74**, 189 (1980).
- [9] H. G. Schuster, *Deterministic Chaos* (VCH, Weinheim, Germany, 1989).
- [10] R. Richter, J. Peinke, W. Clauss, U. Rau, and J. Parisi, *Europhys. Lett.* **14**, 1 (1991).
- [11] A. M. Kahn, D. J. Mar, and R. M. Westervelt, *Phys. Rev.* **45**, 8342 (1992).
- [12] D. Y. Tang, J. Pujol, and C. O. Weiss, *Phys. Rev. A* **44**, R35 (1991).
- [13] Y. Ono, K. Fukushima, and T. Yazaki, *Phys. Rev. Lett.* **52**, 4520 (1995).
- [14] M. Dubois, M. A. Rubio, and P. Berge, *Phys. Rev. Lett.* **51**, 1446 (1983).
- [15] E. Ott, *Chaos in Dynamical Systems* (Cambridge University Press, Cambridge, 1993).
- [16] H. Kodama, S. Sato, and K. Honda, *Phys. Lett. A* **157**, 354 (1991).
- [17] E. R. Clark and E. L. Clark, *Am. J. Anat.* **49**, 441 (1932).
- [18] A. T. Chaytor, W. H. Evans, and T. M. Griffith, *J. Physiol. (London)* **503**, 99 (1997).
- [19] J. M. Ottino, in *Applied Chaos*, edited by J. K. Kim and J. Stringer (John Wiley, New York, 1992), p. 143.
- [20] D. Parthimos, D. H. Edwards, and T. M. Griffith, *Cardiovasc. Res.* **31**, 388 (1996).